Radio Frequency Attenuation by Rocket Plume From Ground Study to In-flight Prediction

Éva Dieudonné, Abelin Kameni, Lionel Pichon, David Monchaux

Radio Frequency Attenuation by Rocket Plume From Ground Study to In-flight Prediction

Éva Dieudonné[1,2], Abelin Kameni[1], Lionel Pichon[1] and David Monchaux[2]

[1] CentraleSupélec, Univ. Paris-Sud, Université Paris-Saclay,
Sorbonne Universités, UPMC Univ Paris 06
3 & 11, rue Joliot-Curie, Plateau de Moulon 91192 Gif-sur-Yvette CEDEX, France
evadieudonne@outlook.fr, abelin.kameni@geeps.centralesupelec.fr, lionel.pichon@geeps.centralesupelec.fr

[2] CNES-DLA | Centre National d'Études Spatiales - Direction des lanceurs
52, rue Jacques Hillairet 75612 Paris CEDEX, France
david.monchaux@cnes.fr

Abstract — Radio frequency communication between the space launcher and the mission control are unusually disturbed by the exhaust plume present in rocket engines. This paper presents the computation of radio wave propagation through the exhaust plume. Thus, frequency-domain finite element method and time-domain discontinuous Galerkin method are implemented for computations in case of a ground domain experiments. Numerical results compared to those obtained from ground experiment show good approximation of the propagation through the plasma over a wide frequency band. For the launcher in flight, an asymptotic method is proposed and has the advantage to give a fast evaluation of the scattering solution. In this case, the exhaust plume area is considered as a perfectly conducting trapezium whose parameters are extracted from the distribution of the plasma permittivity. Results related to the asymptotic method appear to be in good agreement with results based on the full wave approaches.

Index Terms — Asymptotic method, electromagnetic, finite element, plasma, rocket plume, scattering.

I. INTRODUCTION

During a space flight, it is crucial to ensure and maintain the radio frequency (RF) communications between the launcher and the mission control. The high quality reception of radio waves is very important to guarantee security during the flight. Unfortunately, the propagation of emitted and received waves is disturbed by the exhaust plume of the launcher. Corrective measures can be established but are expensive. So, the interest of a sufficiently accurate predictive model is obvious.

The exhaust plume from the space launcher is inhomogeneous plasma whose behavior can be studied through computational fluid dynamic (CFD) models described by Navier-Stokes's and Vlasov's equations [1–4]. The plasma characteristics such as the permittivity, the collision frequency and the plasma frequency are deduced from those CFD models. Generally a frequency dependence of the permittivity is assumed and introduced in the Maxwell's equations whose resolution allows determining attenuation of RF transmission.

Today, only few works are dedicated to study RF transmission during a space flight [5–8]. The Kinefuchi team's has proposed to compute attenuation of RF waves with the plume in the cases of the ground experiment and the launcher in flight [5, 9, 10]. These works deal with all problems of jet impact on radio communications by addressing both, the chemical reactions within the engine, the CFD analysis of the plasma, and the electromagnetic interaction. The Fromentin-Denozière team's works also combine these different aspects to describe the electromagnetic signature of rocket engine plumes [8]. In this paper, aerothermochemical properties of the plume are computed and electromagnetic signature is obtained thanks to the study of the wave reflected by the plasma.

In these studies, numerical models of electromagnetic interaction are based on Finite Difference Time Domain method (FDTD). The computational domain is formed by the plasma whose shape has an important impact on the results. In case of simple shapes of the plasma, the FDTD method gives satisfactory results. Unfortunately practical rocket plumes are of arbitrary shape and the use of a staircase mesh in FDTD method may lead to significant errors.

Numerical calculation in 3D need RAM intensively and are time consuming. In [5] it was shown that 2D calculations are sufficient for the description of physical phenomena. In a 2D approach the electric field has only one component (out of plane component, z-component). However high frequency calculations corresponding to the case where the wavelength is small compared to the size of the plasma region still leads to heavy computational costs. It is why, in this case, an asymptotic method can be used for the prediction of the far field. Such diffraction method has been described in [11]. It considers that the far field scattered by the plasma is similar to the far field scattered by a perfectly conducting trapezium.

In this paper the attenuation of the radio frequency communication by a rocket plume of a spatial launcher is studied with 2D different methods. Two numerical discretization techniques are used for the computations: a frequency domain finite element method and a time domain discontinuous Galerkin method. Both of these methods are suited for unstructured meshes able to take into account arbitrary shapes of the rocket plume. They provide adequate tools for lowest frequencies. For high frequencies an asymptotic method has been developed using [12–14] and considers the plasma as a perfect conducting trapezium whose geometrical parameters are deduced from the distribution of permittivity.

The plasma is characterized by a frequency dependent permittivity given by the Drude relation:

$$\varepsilon_r(\omega) = 1 - \frac{\omega_p^2}{\omega(\omega - i\nu_e)}, \quad (1)$$

where ν_e is the electron collision frequency (s^{-1}), ω_p the plasma frequency (s^{-1}) and ω the frequency ($\omega = 2\pi f$, s^{-1}). The electron collision frequency is the probability of collision between an electron and another species. The plasma frequency describes the frequency at which the electron density varies in the plasma.

$$\omega_p = \sqrt{\frac{N_e q_e^2}{\varepsilon_0 m_e}}, \quad (2)$$

where N_e is electron density (m^{-3}), q_e is elementary electric charge (1.602×10^{-19} A·s), m_e is mass of an electron (9.109×10^{-31} kg), and ε_0 is permittivity of vacuum ($(36\pi \times 10^9)^{-1}$ $s^4 \cdot A^2 \cdot kg^{-1} \cdot m^{-3}$).

In this work, both cases regarding a ground experiment and the launcher in flight are studied. For the ground experiment, the plasma shape is a cylinder. For the launcher in flight, ν_e and ω_p are extracted from a map given in [5].

This paper is organized as follows: Section II presents the ground configuration. This configuration validates the numerical methods and gives first information about plasma properties. Section III presents the numerical methods used in ground configuration for the in-flight estimation. This section also presents an asymptotic method for a fast estimation of the in-flight attenuation.

II. GROUND EXPERIMENT

A. Configuration study

The ground experiment carried out by Kinefuchi team consists of two antennas placed on each side of a jet engine as in Fig. 1.

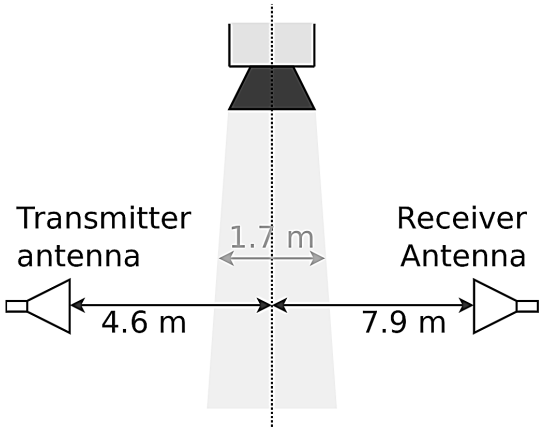

Fig. 1. Kinefuchi antenna setup in ground experiment (Figure 2 in [10]).

A source antenna is placed at a distance 4.6 m and a receiving antenna is placed at 7.9 m. The thickness of the plasma is 1.7 m. The field is recorded versus time in order to divide the engine firing period into periods with distinct electromagnetic properties. Three periods can be observed: Early period, Middle period and Last period. The normalized diffracted field is obtained by the ratio between z-component of electric field E in the presence of the plasma and z-component of electric field E_0 without plasma: $|E/E_0|$ (Table 3 in [10], Table 2).

The method used in Kinefuchi works to estimate the parameters ν_e and ω_p, from experimental results is not described in [10]. In this work, we propose a method to obtain our own homogeneous parameters ν_e and ω_p.

Let define the attenuation L_{dB} (in dB) from the normalized scattered field E/E_0 as:

$$L_{dB} = -20\log_{10}\left(\left|\frac{E}{E_0}\right|\right). \quad (3)$$

Assuming that the plasma is a layer of thickness y, reflection is negligible compared to attenuation and under normal incident wave, it is possible to express E/E_0 in the following form:

$$\frac{E}{E_0} = \exp\left(-i\frac{\omega}{c}\sqrt{\varepsilon_r}y\right). \quad (4)$$

So L_{dB} can be written in this form (in m·s^{1}), even if $\omega_p^2/(\omega^2+\nu_e^2)$ is smaller than 1:

$$L_{dB} = \frac{20\log(e)}{c}\frac{q_e^2}{\varepsilon_0 m_e}\frac{1}{2}\left(\frac{N_e\nu_e y}{\omega^2+\nu_e^2}\right), \quad (5)$$

$$L_{dB} = 4.6\times10^{-5}\left(\frac{N_e\nu_e y}{\omega^2+\nu_e^2}\right). \quad (6)$$

This expression can be found in [2] (equation 14) in cm^2·s^{-1}.

The curve $1/L_{dB}$ as a function of ω^2 is linear [15],

$$\frac{1}{L_{dB}} = \left(\frac{1}{4.6\times10^{-5}N_e\nu_e y}\right)\omega^2 + \left(\frac{\nu_e^2}{4.6\times10^{-5}N_e\nu_e y}\right). \quad (7)$$

and it is easy to obtain the parameters ν_e and ω_p from equation (7) where the slop a and the origin b are defined ($1/L_{dB} = a\omega^2 + b$):

$$\nu_e = \sqrt{\frac{b}{a}}, N_e = \frac{1}{4.6\times10^{-5}N_e a y}. \quad (8)$$

So we obtained (Table 1):

Table 1: Our parameters ν_e and ω_p obtained from the curve $1/L_{dB}$

	Early	Middle	Last
ν_e ($\times10^9$ s^{-1})	38.22	78.35	107.53
ω_p ($\times10^9$ s^{-1})	5.16	6.92	11.74

Our results of $\omega_p$and ν_e are close to those given in Table 2 in [10]. The value of ν_e in Last period is quite different from that given in [10]. The method used in [10] is not defined exactly so it's not possible to know how this value is obtained. However our values of ν_e given a better estimation of the attenuation for the frequency 5.6~GHz and 8.5~GHz (see Section C, Table 2).

B. Numerical modeling

The plasma is modeled as a cylinder as shown in the configuration given by Fig. 1. A time domain and a frequency domain approaches are used to describe attenuation of RF waves. Both methods use a triangular mesh to discretize more accurately the computational domain.

For the frequency domain computations, a Finite Element Method (FEM) is applied. This approach provides a fast response to a discrete set of frequencies. Many softwares are able to solve Maxwell equations with the finite element method. The commercial software COMSOL already used in our laboratory is employed.

For the time domain computations, a nodal Discontinuous Galerkin (DG) method is applied. The numerical code has been developed in our laboratory. This approach allows determining through one simulation, the RF waves attenuation for a frequency band defined by the transient incident signal. The DG method is suitable for high order spatial elements which allow to reduce dispersion error commonly encountered in FDTD methods, and to improve the solutions accuracy.

1) Frequency domain method

The symmetry of the system assumes to use half of the plasma and a Perfect Magnetic Conductor (PMC) boundary condition as shown in Fig. 2. The computational domain is surrounded by a Perfect Matched Layer (PML) of 1 m thickness. The spatial discretization in PML region is 5 elements per wavelength (λ/5) whereas it is 10 elements per wavelength λ/10) elsewhere. The excitation is generated by a dipole located at the point S and the electric field is recorded at the point R.

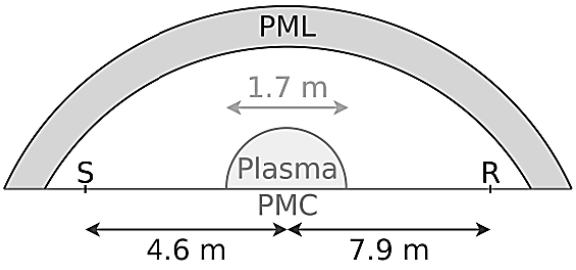

Fig. 2. Box calculation for 2D FEM (not to scale).

2) Time domain method

To easily deal with frequency dependence of the permittivity, the Maxwell-Ampère equation is rewritten in terms of conductivity:

$$\sigma(\omega) = -i\omega(\varepsilon_r - 1)\varepsilon_0. \quad (9)$$

Both Maxwell's equations, formed by the Faraday's law and the inverse Fourier transform of Ampère's law give us the following:

$$\mu_0\frac{\partial\vec{H}}{\partial t} + \vec{\nabla}\times\vec{E} = \vec{0}, \quad (10a)$$

$$\varepsilon_0\frac{\partial\vec{E}}{\partial t} - \vec{\nabla}\times\vec{H} + \sigma(t) * \vec{E} = \vec{0}, \quad (10b)$$

where " $*$ " designed the convolution product of functions $\sigma(t)$ and $\vec{E}(t)$. Note that $\sigma(t)$ is the inverse Fourrier transform of $\sigma(\omega)$ obtained from the vector fitting technique [16] widely used in time domain modeling of dispersive media. The convolution term is computed thanks to an iterative process including the solutions at all the previous time steps [17]. This term is

introduced in time domain computations as an explicit term.

A time domain DG method based on upwind fluxes is assumed in this work. The simulation domain is delimited by an efficient PML recently proposed for time domain scattering problems [18]. In the initial mesh, the spatial discretization is PML region is 0.33 element per wavelength whereas it is 1 element per wavelength elsewhere. Elements of order $p=8$ are used in these computations. In this case the number of nodes in an element is given by $0.5(p+1)(p+2)$.

The simulations consist in propagating a modulated Gaussian pulse with and without the plasma.
This pulse is given by (11) with a frequency band between 0 and 10~GHz.

$$u(t) = \sin(2\pi f_0 t)\exp[-a(t-t_{ho})^2], \qquad (11)$$

where $f_0 = 5.5$ GHz, $a = 2.4 \times 10^{19}$ s^{-1} and $t_{ho} = 7 \times 10^{-10}$ s.

C. Numerical results

Numerical results from FEM and DG computations are compared to those provided by Kinefuchi's works (Table 3 in [10]).We also added a comparison to analytical results obtained from 1D approximation [19] (Plasma is assumed to be a layer with a thickness of 1.7 m) and Mie series [20] (Plasma is assumed to be a circular cylinder with a diameter of 1.7 m). The values obtained from these different methods are presented in Table 2.

Table 2. Comparison of experimental and numerical values of normalized scattered field

Frequency	Method	Early	Middle	Last
2.3 GHz (S-Band)	**Exp**	**0.199**	**0.174**	**0.039**
	FDTD	0.188	0.129	0.102
	1D	0.174	0.187	0.028
	Mie	0.250	0.271	0.147
	FEM	0.250	0.271	0.147
	DG	0.251	0.268	0.141
5.6 GHz (C-Band)	**Exp**	**0.319**	**0.258**	**0.022**
	FDTD	0.310	0.200	0.034
	1D	0.340	0.236	0.037
	Mie	0.303	0.196	0.021
	FEM	0.302	0.195	0.022
	DG	0.308	0.201	0.015
8.5 GHz (X-Band)	**Exp**	**0.519**	**0.300**	**0.063**
	FDTD	0.424	0.241	0.024
	1D	0.510	0.306	0.054
	Mie	0.510	0.298	0.072
	FEM	0.509	0.297	0.073
	DG	0.523	0.318	0.078

The 1D results are very close to the experimental values because this model was used to compute the parameters ω_p and ν_e. The difference is due to the fact that the straight line is not passing by all the points.

Both DG and FEM results are validated by comparison to the Mie solution. Mie solution matches the experimental results except for the low frequency. In fact, the good agreement between numerical and experimental data is due to the validity of homogeneous parameters for high frequencies.

DG method allows obtaining the entire frequency band with one calculation thanks to a Fourier transform of the recorded field. On the other hand, the FEM requires a calculation of each frequency. We display all the results on a graph versus frequency for comparison (Fig. 3).

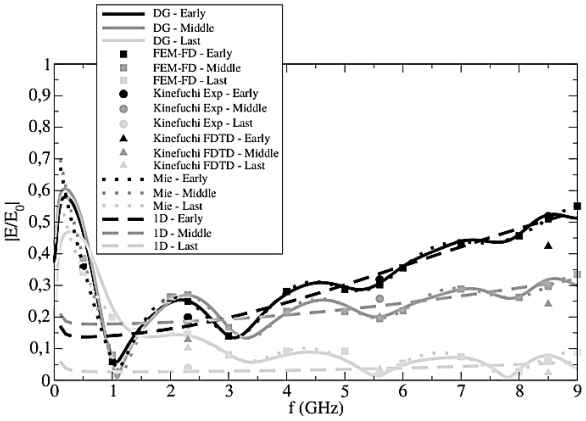

Fig. 3. Comparison of calculation methods for the normalized scattered field versus the frequency.

The mean error calculation (relative to Mie) shows errors less than 1% for Early and Middle with FEM and less than 8% with DG. The error is greater for the Last period, less than 5\% for FEM and less than 18\% for DG. The high error obtained by the DG method is due to the increase of the relative error observed at low frequencies.

It is also observed that DG, FEM, Mie converge to the 1D solution when the frequency increases. This convergence shows that homogeneous parameters are even more acceptable if the frequencies are high. Therefore, high frequencies assumptions made in the 1D method, may allow obtaining a better estimation of the parameters for 2D calculations.

The methods studied for the ground configuration will be used by CNES in future work to validate CFD models.

III. IN-FLIGHT ATTENUATION ESTIMATION

In this section the finite element method in frequency domain (FEM) and an asymptotic method based on the diffraction theory are used to calculate

attenuation of RF waves during a flight. In the asymptotic method the plume geometry is considered as a trapezium. The advantage of such approach is to avoid a memory-intensive calculation FEM and to allow a fast estimation of the attenuation. The main difficulty is the choice of the trapezium parameters. In this work we propose a new method TIP[3] (Trapezium Isovalues Permittivity Predict Parameter) to derive these parameters from a map of the permittivity.

A. Configuration study

The rocket studied in this work is the second stage of the MV5 launcher flight at 85 km of altitude [5]. A look angle τ is introduced to describe the configuration at each altitude (Fig. 4).

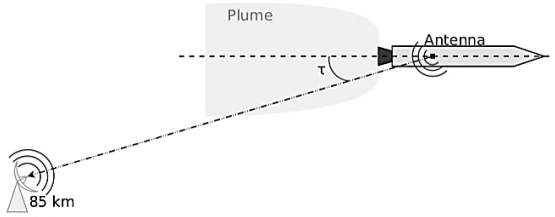

Fig. 4. In-flight configuration. Launcher fly at 85 km of the ground antenna, τ is the look angle (Figure 1 in [5]).

Kinefuchi team performed CFD calculation deriving a map of ω_p and ν_e. Maps of ω_p and ν_e are extracted from Figure 17 in [5] with a numerical code developed in MatLab and incorporate in FEM calculation (Fig. 5).

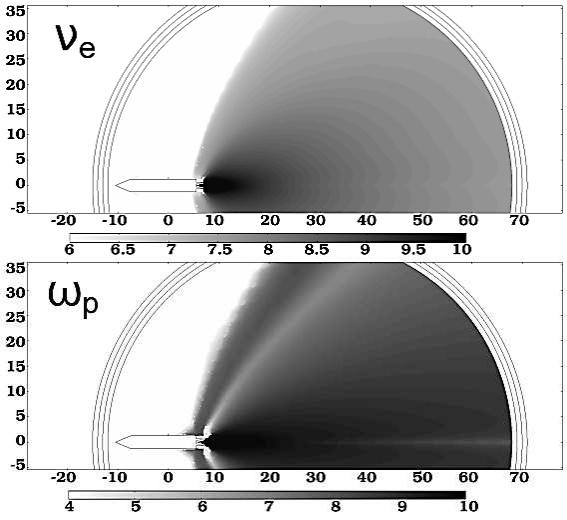

Fig. 5. Map of $\log_{10}(\omega_p)$ and $\log_{10}(\nu_e)$ in calculation domain.

In-flight measurement of the attenuation L_{dB} is carried out at the frequency 300~MHz (Figures 22 and 23 in [5], grey points in Fig. 7).

B. 2D Finite Element Method

The calculation domain is represented in Fig. 6.

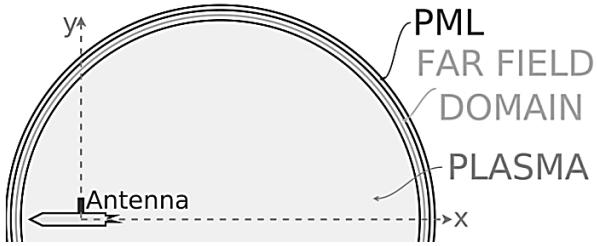

Fig. 6. Geometrical representation. Radiuses of the arc are 40 m, 41 m, 42 m and 43 m.

The far-field calculation is used for reducing the size of the computational domain, because attenuation is measured at 85 km of the launcher.

A cardioids antenna is placed at $x = 7$ m of the nozzle exit and at $y = 1.25$ m (radius of launcher) of the launcher middle.

The spatial discretization is 10 elements per wavelength (λ/10) and the domain is surrounded by a PML. The attenuation (in dB) is calculated and shown in Fig. 7.

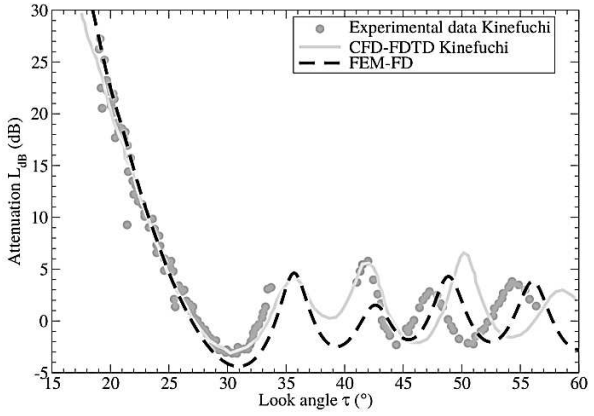

Fig. 7. Attenuation obtained by FEM.

A good agreement is observed between FEM and experimental data. The differences might be due to the poor quality of map of ω_p and ν_e resulting from the literature.

We perform simulations in frequency domain using the FEM method. The attenuation curves versus the look angle τ are shown for different frequency values in the Fig. 8.

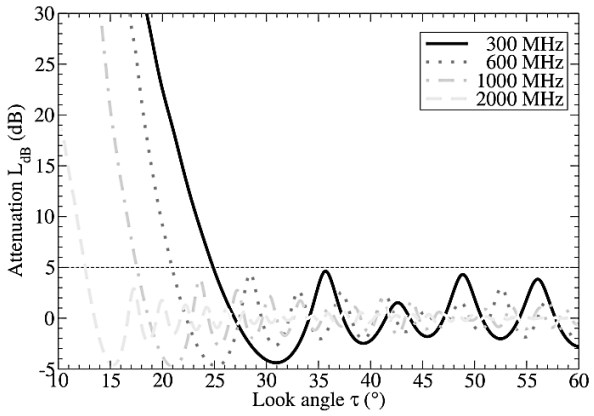

Fig. 8. Attenuation in dB obtained by the FEM method for different frequency values.

These curves present a similar behavior. We remark a shift of the first minimum. After this first minimum, attenuations remain below 5 dB. So even if the global curve is not correctly fitted, a good prediction of this minimum constitutes an interesting result. A statement of the look angle τ_{min} for which the first minimum occurs is shown in Fig. 13 (black points).

A linear regression (black curve in Fig. 13) is achieved and it shows a very good correspondence (all points are on the function): equation (12).

$$\tau_{min} = -84.80 + 115.75\lambda^{0.075}. \qquad (12)$$

This equation allows an immediate obtaining of τ_{min} for any frequency between 200 MHz and 2 GHz.

C. Diffraction by trapezoidal perfect conductor

We propose in this section an asymptotic method for the prediction of the far field. The numerical code is developed in MatLab software. Trapezium parameters are defined in Fig. 9.

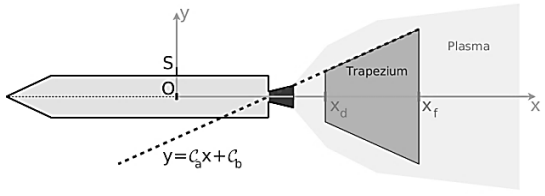

Fig. 9. Trapezium characteristics.

The objective is obtaining the trapezium characteristics directly from the permittivity. For beginning, the trapezium published in Kinefuchi's works [5] which have these properties is considered: $x_d = 20$ m, $x_f = 64$ m, $C_a = 0.43$ and $C_b = -2.61$. This trapezium is deduced to flight measurements. Unfortunately the in-flight measures are quite difficult to get.

That is why the trapezium parameters are extracted from the map of the permittivity. So we compared the trapezium of Kinefuchi [5] and the cartography of permittivity (Fig. 10).

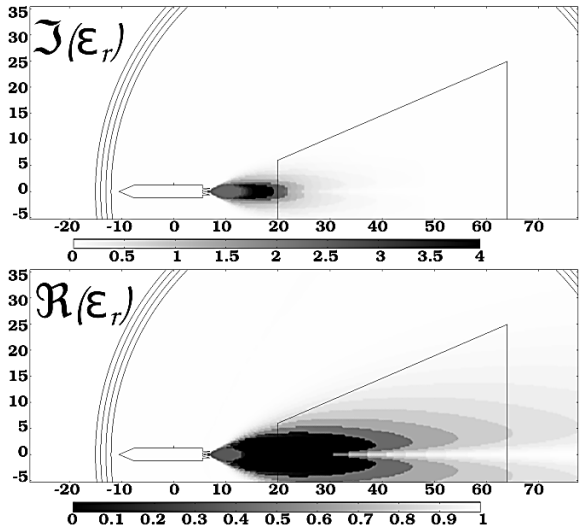

Fig. 10. Comparison between Kinefuchi trapezium and permittivity.

We observed that the basis of the trapezium near to the launcher corresponds to value 2.5 in the representation of $\Im(\varepsilon_r)$. We also observed that the basis of the trapezium far to the launcher corresponds to value 0.85 in the representation of $\Re(\varepsilon_r)$.

Isovalues of $\Im(\varepsilon_r) = 2.5$ and $\Re(\varepsilon_r) = 0.85$ are drawn and the correspondence between the adapted trapezium and the trapezium defined by these isovalues are confirmed (Fig. 11).

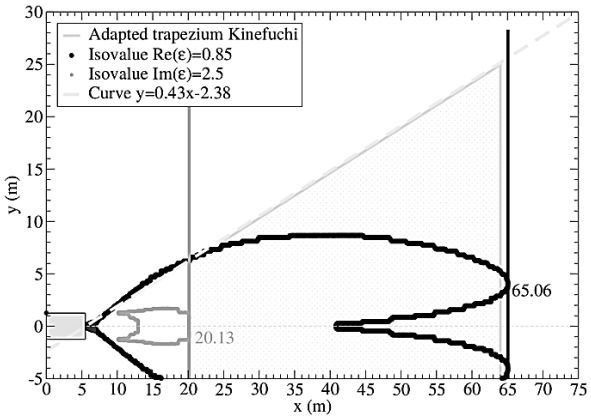

Fig. 11. Comparison between the trapezium of Kinefuchi and the trapezium defined by isovalues of the permittivity.

The maximum values of x for isovalues $\Im(\varepsilon_r) = 2.5$ and $\Re(\varepsilon_r) = 0.85$, give x_d and x_f. The slope of the trapezium is determined by the line passing through the center of the throat and the end of the nozzle, so $C_a = 0.43$ and $C_b = -2.38$.

This method is generalized to all frequencies. x_d and x_f for all frequencies are determined with the use of the isovalues like made for 300 MHz. Fig. 12 shows the variations of x_d and x_f versus wavelength and linear regression.

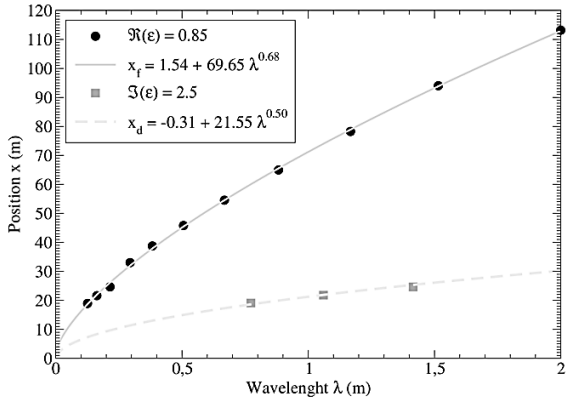

Fig. 12. x_d and x_f versus wavelength and linear regression.

The values x_d and x_f is given by:

$$x_d = -0.31 + 21.55\lambda^{0.50}, \quad (13)$$

$$x_f = 1.54 + 69.65\lambda^{0.68}. \quad (14)$$

The method TIP^{3}c is defined. This method gives the trapezium parameters: x_d by equation (13), x_f by equation (14), $C_a = 0.43$ and $C_b = -2.38$.

TIP^{3}c shows a significant difference in τ_{min} (Fig. 13) compared to FEM. The method TIP^{3}p is defined to correct that. This method gives the trapezium parameters: x_d by (13), x_f by equation (14), C_a by equation (15) and $C_b = -2.38$.

$$C_a = 0.06 + 0.39\lambda^{0.23}. \quad (15)$$

The values τ_{min} for methods TIP^3 and FEM are shown in Fig. 13.

Light-grey curve (TIP^{3}c) corresponds to black curve (FEM) with an error less than 5% in $\lambda = [0.565 - 1.090]$ m. So the value $C_a = 0.43$ given by the geometry of the nozzle is correct for this frequency range. It's interesting to remark that the half of the nozzle opening (0.65 m) is included to this range. Grey curve (TIP^{3}p) has an error less than 5% up to $\lambda = 0.037$ m and also an error less than 1% up to $\lambda = 0.1$ m.

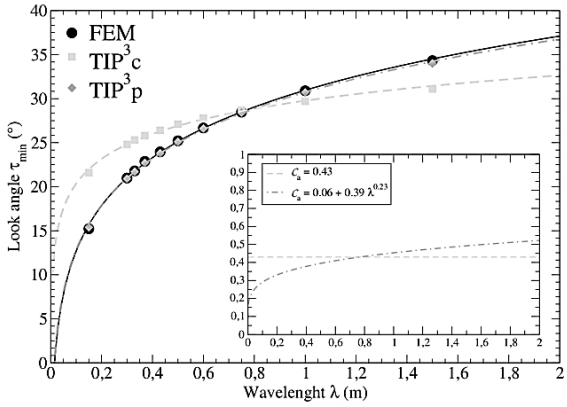

Fig. 13. τ_{min} (dots: exact values and line: linear regression). Expression of C_a.

Some attenuation curves obtained from the FEM and the asymptotic methods using TIP^{3}p are shown in Fig. 14.

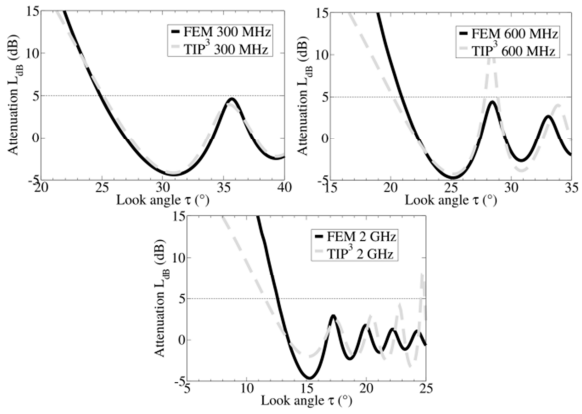

Fig. 14. Attenuation at 300 MHz, 600 MHz and 2 GHz.

A good angular behavior is reproduced by the TIP^{3}p method. Nevertheless an overestimation of the attenuation after the first minimum τ_{min} is noted for frequency values beyond 600~MHz. The FEM computations show that this attenuation is smaller than 5 dB for greater angles than τ_{min}. With the TIP^{3}p method, the variations of attenuation more than 5 dB can be ignored for the angles greater than τ_{min}.

Fig. 15 shows $\log_{10}(E/E_0)$ in plasma and TIP^{3}p perfectly conducting trapezium cases.

Interference fringe corresponding to the first minimum follow the slope of the trapezium. The trapezium serves as a mask increasing attenuation in the shadow. However the reflection at the corner of the trapezium scatters the field in the shadow of the trapezium thus modifying the slope of the attenuation for a low angle. The position of the bases causes the first interference fringe to follow the slope of the trapezium.

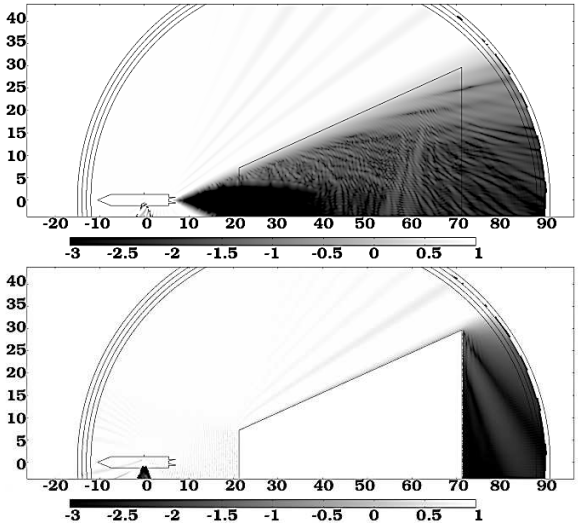

Fig. 15. Comparison between normed electric field in presence of the plasma and the normed electric field in presence of the TIP^{3}p perfectly conducting trapezium at 300 MHz ($\log_{10}$).

IV. CONCLUSION

In this paper the radio-frequency communication attenuation through a plasma rocket plume was studied using different methods.

The analysis of the ground experiment revealed the importance of the attenuation phenomena through the plasma. A frequency-domain finite element method (FEM) and a time domain discontinuous Galerkin method (DGTD) provided a good estimation of the attenuation. DGTD allows unstructured meshes while providing a frequency response over a wide frequency band using a transient excitation. FEM gives a fast response for a discrete set of frequencies. The ground experiment gives an estimate of the parameters of the plasma and validates the calculation tools (CFD and FEM) in order to deduce the attenuation in-flight.

In the case of the launcher in flight, attenuation of RF communications is computed by the FEM method using maps of ν_e and ω_p from the literature. To face problem of the heavy computational time that occurs with FEM approach for high frequencies, an asymptotic technique is presented. It is proposed when the shape of the plume is considered as a trapezium whose parameters are deduced from the knowledge of the permittivity distribution (TIP^{3}p). A complete validation was proposed for a wide range of frequency values. The numerical method dedicated to the diffraction by a perfectly conducting trapezium associated with the method TIP^{3}p allows a rapid estimation of the attenuation in-flight.

REFERENCES

[1] R. R. Mikatarian, C. J. Kau, and H. S. Pergament, “Fast computer program for nonequilibrium rocket plume predictions”, AeroChem TP-282, (1972).

[2] L. D. Smoot, and D. L. Underwood, “Prediction of microwave attenuation characteristics of rocket exhausts”, AIAA 6th solid propellant rocket conference, 65-181, (1965).

[3] L. D. Smoot, and T. J. Seliga, “Rocket exhaust plume radar attenuation and amplitude/phase noise”, J. Spacecraft, 4, pp.774–780, (1967).

[4] J. A. Blevins, R. A. Frederick, and H. W. Coleman. “An assessment of microwave measurement techniques in rocket exhaust applications”, 32nd aerospace sciences meeting & exhibit, 94-0671, (1994).

[5] K. Kinefuchi, K. Okita, I. Funaki, T. Abe, “Prediction of in-flight radio frequency attenuation by a rocket plume by applying CFD/FDTD coupling”, 49th AIAA/ASME/SAE/ ZSEE Joint Propulsion Conference, 2013-3790, (2013).

[6] L. Glen McMillion, “A simple method for predicting RF attenuation through a rocket exhaust plume”, U.S. Army Research Office, (1997).

[7] B. Van der Veek, S. Chintalapati, D. R. Kirk, H. Gutierrez, and R. F. Bun, “Modeling and validation of Ku-band signal attenuation through rocket plumes”, Journal of Spacecraft and rockets, 50, pp.992–1001; (2013).

[8] B. Fromentin-Denozière, D. Gueyffier, and J. Simon, “Numerical modelling of the radar signature of rocket exhaust plumes”, International Conference on Electromagnetics in Advanced Applications (ICEAA 2012), pp.400–403, (2012).

[9] K. Kinefuchi, I. Funaki, and T. Abe, “Frequency-dependent FDTD simulation of the interaction of microwaves with rocket-plume”, IEEE Transactions on antennas and propagation, 58, pp.3282–3288, (2010).

[10] K. Kinefuchi, I. Funaki, H. Ogawa, T. Kato, S. Tachikawa, T. Shimada, and T. Abe, “Investigation of micromawe attenuation by solid rocket exhausts”, 47th AIAA Aerospace Science Meeting and Exhibit, 2009-1386, (2009).

[11] K. Kinefuchi, I. Funaki, and T.~Abe, “Prediction of in-flight frequency attenuation by rocket plume applying diffraction theories”, Journal of spacecraft and rockets, 50, pp. 150–158, (2013).

[12] J. H. Whitteker, “Diffraction over flat-topped terrain obstacle”, IEE proceedings, 137, (1990).

[13] G. Millington, R. Hewitt, and F. S. Immirzi, “Double knife-edge diffraction in field-strength predictions”, Proceedings IEE, 507, (1962).

[14] G. Millington, R. Hewitt, and F. S. Immirzi, “The Fresnel surface integral”, Proceedings IEE, 508, (1962).

[15] K. M. Mphale, P. V.C. Luhanga, and M. L. Heron, “Microwave attenuation in forest fuel flames”, Combustion and flame, 154, pp.728-739, (2008).
[16] B. Gustavsen, and A. Semlyen, “Rational approximation of frequency domain responses by vector fitting”, IEEE Trans. Power Delivery, 14, pp.1052–1061, (1999).
[17] M. Boubekeur, A. Kameni, L. Bernard, A. Modave, and L Pichon, “3-D Modeling of Thin Sheets in the Discontinuous Galerkin Method for Transient Scattering Analysis”, IEEE Trans. Magn., 50, pp. 493–496, (2014).
[18] A. Modave, A. Kameni, J. Lambrechts, E. Delhez, L. Pichon, and C. Geuzaine, “An optimum PML for scattering problems in the time domain”, Eur. Phys. J. Appl. Phys., 64, pp.24502, (2013).
[19] É. Dieudonné, N. Malléjac, C. Amra, and S. Enoch, “Surface and bulk scattering by magnetic and dielectric inhomogeneities: a first-order method”, J. Opt. Soc. Am. A, 30, pp. 1772–1779, (2013).
[20] J. Van Bladel, *Electromagnetic Fields*, John Wiley & Sons, pp. 743, (2007).